Microthermometric study of fluids associated with Pb-Zn mineralization in the vicinity of the Pine Point mining camp

W.A. Turner[1]

Abstract: A regional study undertaken south and west of Great Slave Lake, Northwest Territories, focused on evaluating the fluids associated with lead-zinc mineralization in the Pine Point mining camp. Microthermometric studies identified two fluid types: Type 1 fluid was observed in sphalerite and dolomite, and is a moderately low-temperature (respective ave. 86 and 100°C), high-salinity calcic brine (ave. 25 to 27 wt. % $CaCl_2$-NaCl), that was directly involved in the processes that deposited the metals; Type 2 fluid, observed in calcite and celestite, is slightly lower in temperature (~85°C), is less saline (ave. ~9 wt. % $CaCl_2$-NaCl), and was not involved in metal deposition.

Résumé : Une étude régionale effectuée au sud et à l'ouest du Grand lac des Esclaves, dans les Territoires du Nord-Ouest, portait sur l'évaluation des fluides associés à la minéralisation en plomb-zinc dans le camp minier de Pine Point. Des études microthermométriques ont permis d'identifier deux types de fluides : le fluide de type 1, observé dans de la sphalérite et de la dolomite, est constitué d'une saumure calcique à salinité élevée (pourcentage massique moyen de $CaCl_2$ et NaCl de 25 à 27 %) et à température modérémment faible (moyenne respective de 86 EC et de 100 EC), qui a contribué directement aux processus de dépôt des métaux; le fluide de type 2, observé dans de la calcite et de la célestine, a une température légèrement plus faible (env. 85 EC), est moins salin (pourcentage massique moyen de $CaCl_2$-NaCl d'environ 9 %) et n'a pas contribué au dépôt des métaux.

[1]C.S. Lord Northern Geoscience Centre, P.O. Box 1500, Yellowknife, NWT, X1A 2R3, allan_turner@gov.nt.ca; cslord_centre@gov.nt.ca*

* Now at Elemental Geological Services Ltd., 9143-71 Ave., Edmonton, Alberta, T6E 0V9, allan_turner@telus.net

INTRODUCTION

The C.S. Lord Northern Geoscience Centre examined the fluids responsible for ore and gangue mineral precipitation from selected localities to the south and west of Great Slave Lake, southern Northwest Territories. This study is part of a Targeted Geoscience Initiative (project # 232-110-010009) titled "Potential for carbonate-hosted Pb-Zn (MVT) deposits in northern Alberta and southern NWT"; a collaborative project between C.S. Lord Northern Geoscience Centre, the Geological Survey of Canada, and the Alberta Geological Survey (Hannigan 2001, 2002; Hannigan et al., 2002). The goals of the multidisciplinary project are to delineate the distribution and describe the origin of known Mississippi Valley-type lead-zinc deposits in the Pine Point mining camp and to investigate the potential for further undiscovered lead-zinc orebodies in northern Alberta and southern Northwest Territories. The fluid study described herein is one component of the MVT project.

The primary goal of this study was to constrain the trapping temperatures and salinities of fluids associated with the ore and gangue minerals. To accomplish this goal, nondestructive microthermometric analyses of fluid inclusions were conducted. The study area ranges from the Little Buffalo River in the east to Heart Lake in the west and from Falaise Lake in the north to Escarpment Lake in the south (Fig. 1, 2).

REGIONAL GEOLOGICAL SETTING

The area of study focuses on the northeastern section of the Interior Platform, a relatively undisturbed sedimentary sequence, in the southern Northwest Territories (Fig. 1; Douglas et al., 1970). The Phanerozoic stratigraphic section comprising the Interior Platform thickens to its western border with the Cordillera foreland. To the east it thins to an erosional edge that exposes Precambrian rocks of the Canadian Shield. Within the study area, the Interior Platform hosts the Presqu'ile barrier, a carbonate reef complex that formed during the Givetian Age of the Middle Devonian (Rhodes et al., 1984). The Presqu'ile barrier outcrops on the southern shores of Great Slave Lake (Fig. 1), and regionally dips to the west at 1.9 m per km (Rhodes et al., 1984). This barrier extends to the southwest for approximately 400 km, and varies between 20 and 90 km in width (Qing and Mountjoy, 1994). Development of the Presqu'ile barrier restricted seawater circulation, giving rise to evaporite deposits and lesser carbonate units to the south in the Elk Point Basin (Fig. 1).

Regional stratigraphy

Several authors have described the stratigraphy south of Great Slave Lake. A brief review is presented below and the reader is referred to references cited for more information.
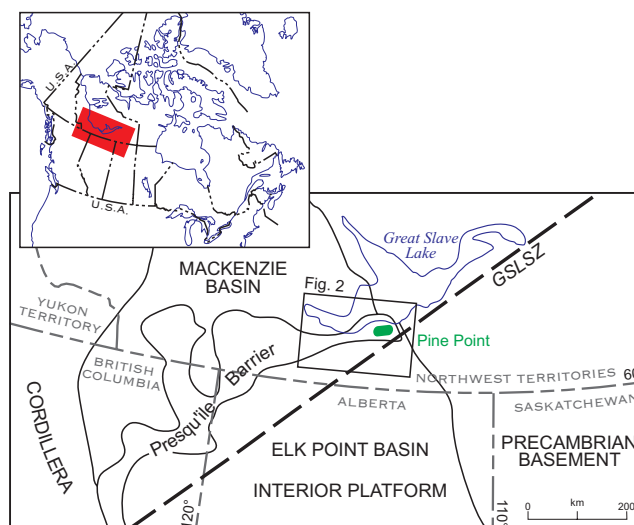

Figure 1. Simplified map of Devonian geology, northwestern Canada showing the location of the Presqu'ile barrier with respect to the Mackenzie and Elk Point basins. *Modified after* Qing and Mountjoy (1994) and Turner and Gal (2003). GSLSZ = Great Slave Lake Shear Zone.

The Proterozoic basement in the Pine Point area is unconformably overlain by siliciclastic rocks of the Old Fort Island Formation, and carbonate deposits and siliciclastic rocks of the Mirage Point Formation, both of which are interpreted as Ordovician or older in age (Douglas, 1959; Belyea and Norris, 1962; Norris, 1965). Unconformably overlying the Mirage Point Formation are carbonate units of the Chinchaga Formation, which is lower Middle Devonian (Eifelian) in age (Norris, 1965).

The Presqu'ile carbonate barrier buildup and its associated lithologies have been studied by Law (1955), Belyea and Norris (1962), Richmond (1965), Norris (1965), Skall (1975), Rasmussen (1981), Lantos (1983), Rhodes et al. (1984), and Norris and Uyeno (1998), among others. The rocks conformably overlie the Chinchaga Formation, and represent five paleoenvironments. These environments are as follows: 1) the Keg River Formation, which represents the lower carbonate platform; 2) a carbonate barrier complex, composed of lower and upper sections termed the Pine Point and Sulphur Point formations; 3) the evaporitic sequence of the Muskeg Formation that is equivalent to a back-barrier environment; 4) the Buffalo River and Windy Point formations, which were deposited to the north of the barrier in a fore-barrier environment; and 5) the Watt Mountain and Slave Point formations, overlying the barrier and its equivalents.

West of the Pine Point area, in the vicinity of the Hay River, is the erosional edge of the Upper Devonian Hay River Formation (Jamieson, 1967). Meijer Drees (1993) further defined this formation to encompass all beds between the top of the Slave Point Formation and the base of the Twin Falls
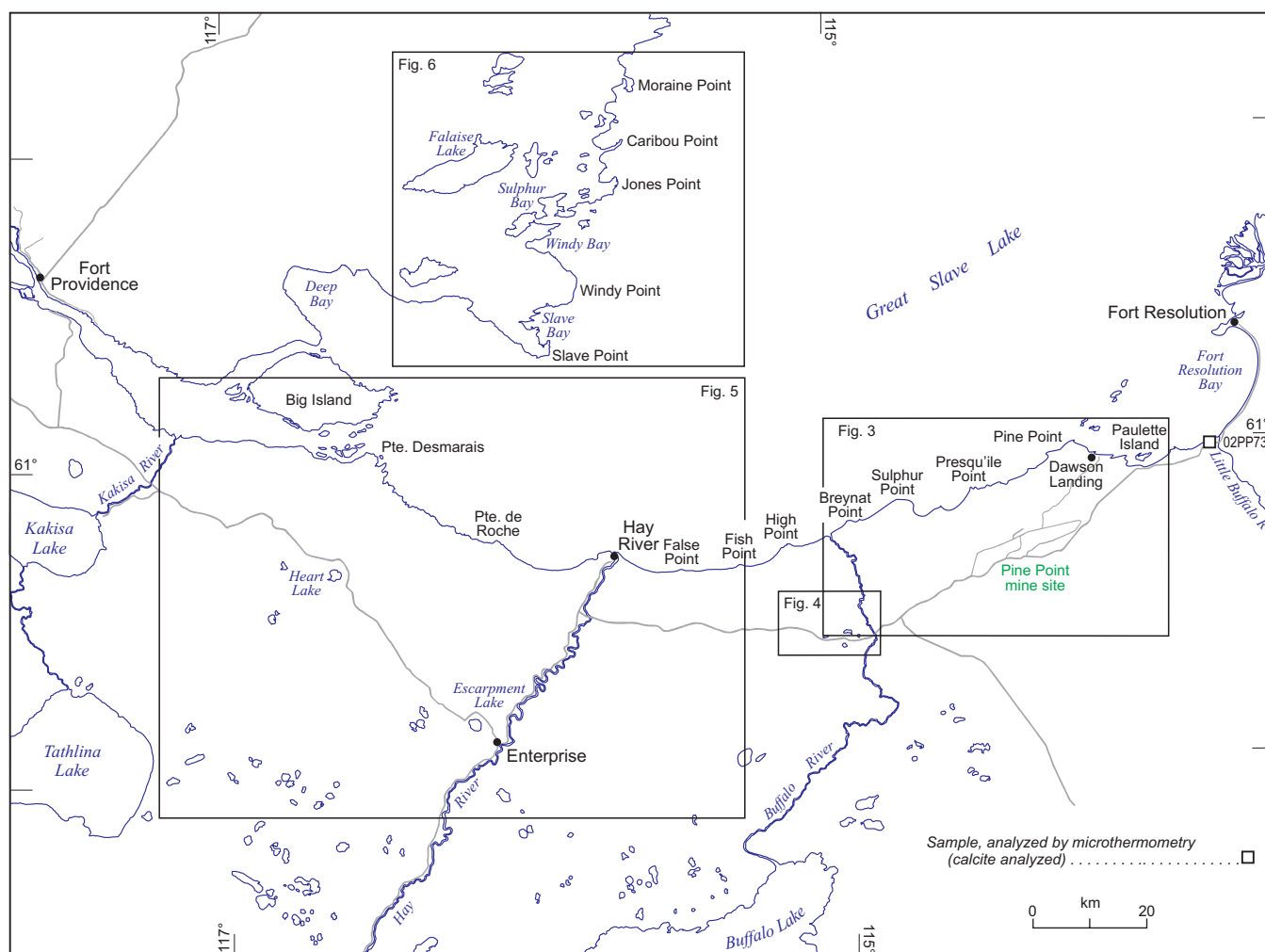
Figure 2. Location map of the study area, showing the four different domains (Fig. 3 to 6).

Formation. The siliciclastic and carbonate lithologies associated with the Hay River Formation, which incorporates the Escarpment Member, and the unconformably overlying Twin Falls Formation, including the Alexandra Member, have been studied by Cameron (1918), Belyea and McLaren (1962), Jamieson (1967), Williams (1977), Hadley (1987), Hadley and Jones (1990), and Bellow (1993). Although these units have been extensively examined, the formal classification of the different lithologies into formation, member and facies status remains under considerable debate.

MINERALIZATION

Exploration drilling carried out at the Pine Point mining camp determined that the orebodies are confined to extensive conduit systems (paleokarsts) that formed in select carbonate facies along the strike of the Presqu'ile barrier complex (Kyle, 1981). Rhodes et al. (1984) proposed that three paleokarst systems exist: two large-scale dissolution channelways oriented at approximately 065° named North and Main trends, and a less continuous channelway termed the South Trend (Fig. 3). To the west of Buffalo River, Westmin Resources Limited (operator of the Great Slave Reef project) conducted extensive drilling along the proposed extension of the Main Trend, and delineated seven orebodies (Randall et al., 1985; Turner et al., 2002; Fig. 4), bringing the total number of known ore deposits between Hay River and Little Buffalo River to over 90. During the mid to late 1970s and early 1980s exploration drilling was carried out to the west of Hay River in the Tathlina (Gulf Minerals Canada Limited; Germundson, 1979, 1980) and Hay West areas (Pine Point Mines Ltd; Fig. 5; Carter, 1980, 1981; Klein, 1981, 1982), and to the north of Hay River in the Windy Point–Qito areas (Pine Point Mines Ltd; Fig. 6; Brabec, 1976, 1981; Heal, 1977; Lane, 1980a). Although zones of hydrothermal dolomite were identified, only sporadic pockets of sulphide mineralization were intersected in drill core during these programs.
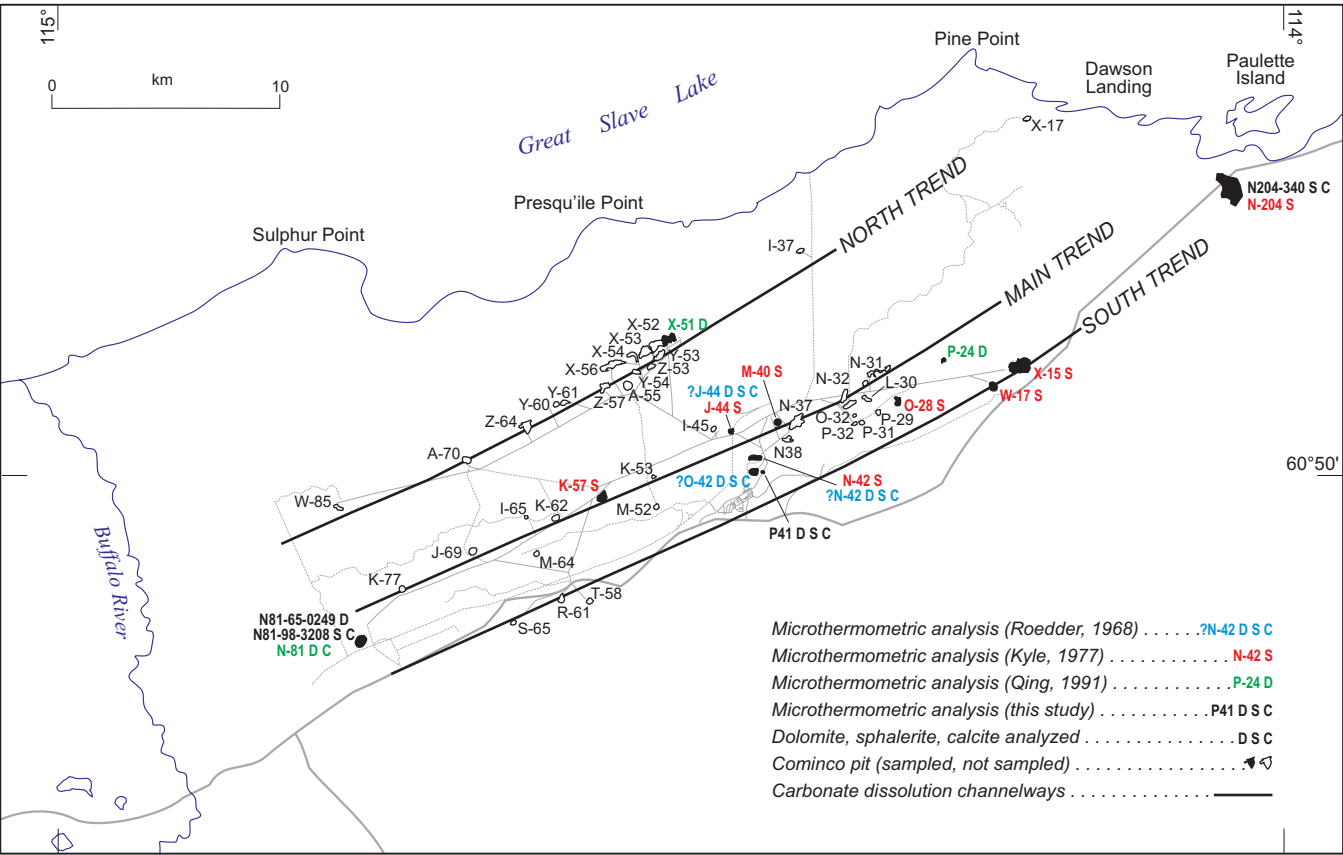
Figure 3. Pine Point mining district showing the locations of the ore deposits in relation to the North, Main, and South trends. The pit locations of the samples studied by fluid inclusion microthermometric analyses are filled, and are labelled appropriately (pit designation, sample identification (this study only), and type of material analyzed, and type of material analyzed; i.e., D= dolomite, C= calcite, S= sphalerite). Figure *modified from* Turner and Gal (2003). *See* Figure 2 for location.

Paragenesis

The alteration and ore mineral assemblages in the Pine Point mining camp have been documented by Skall (1975), Kyle (1977, 1981), Krebs and Macqueen (1984), Rhodes et al. (1984), Qing (1991), and Qing and Mountjoy (1994), among others. The paragenesis of the alteration assemblages is characterized in terms of its relationship to ore emplacement, and is separated into three stages (pre-ore, main event of ore deposition, and post-ore) (Fig. 7).

Pre-ore stage

The first widespread event of dolomitization of the rocks in the Presqu'ile barrier was the recrystallization of limestone to a fine-grained dolostone. This recrystallization event, which occurred during early diagenesis, preserved the textures of fossils and sedimentary structures, allowing for identification of the protolith lithologies.

Following this widespread event of dolomitization, hydrothermal fluids were channelled into select facies within the carbonate barrier, fore-reef, and overlying units,
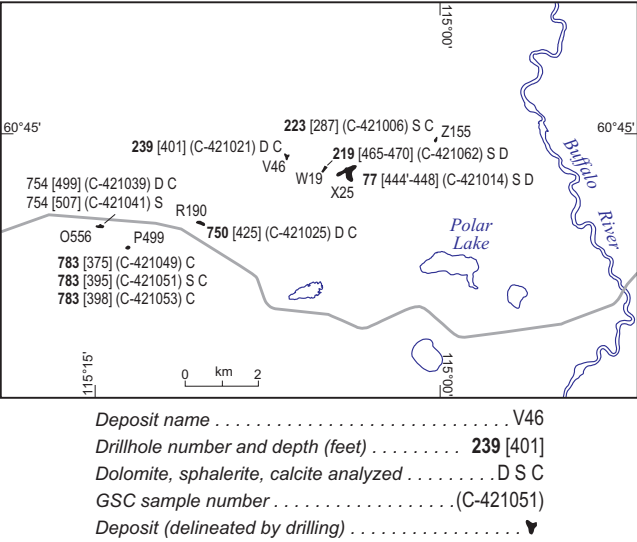
Figure 4. Great Slave Reef (Westmin) project area showing the locations of seven ore deposits. Fluid inclusion microthermometric analyses were conducted on all seven deposits in this study. *See* Figure 2 for location.
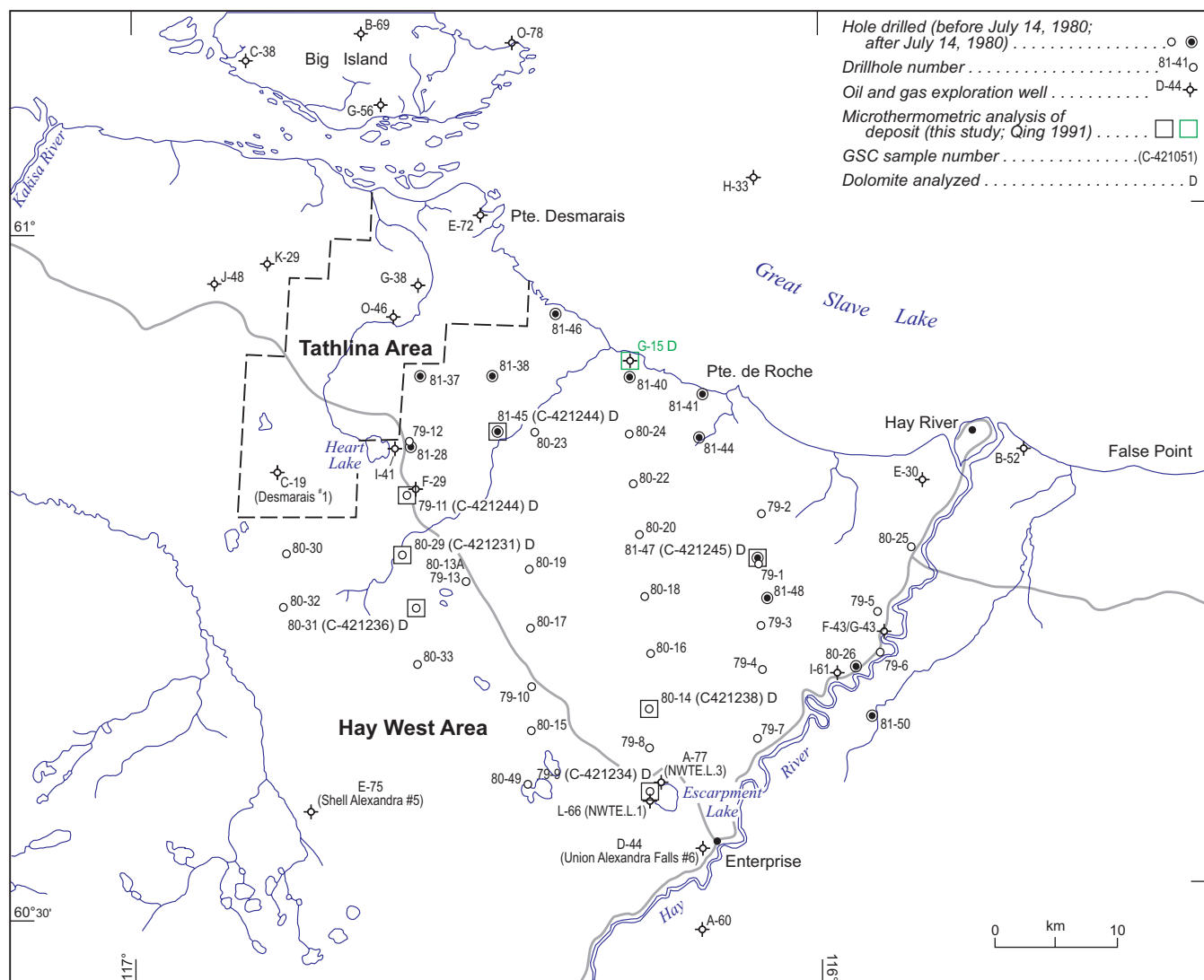
Figure 5. Drillhole locations (drilled by Pine Point Mines Ltd. (owned by Cominco Ltd.) and oil and gas exploration companies) west of Hay River. Fluid inclusion microthermometric analyses on dolomite was conducted on drill cores (indicated by a box around drill core location). Figure *modified after* Klein (1981, 1982). *See* Figure 2 for location.

subsequently causing fracturing and collapse within these units and recrystallization of the fine-grained dolostone to "Presqu'ile" dolostone (Skall, 1975). "Presqu'ile" dolostone is characterized as a coarse-grained dolomite that hosts isolated subrounded concentrations of insoluble residues, typically between 1 and 7 mm in diameter (Skall, 1975; Rhodes et al., 1984). Krebs and Macqueen (1984) proposed that the "Presqu'ile" stage of dolomitization did not occur during a single fluid event, but rather resulted from complex superimposed processes of percolating surficial waters and ascending hydrothermal fluids.

Succeeding the stage of "Presqu'ile" dolostone precipitation, limestone remnants trapped between the dolomitized fissures, fractures, and fragments were dissolved (Krebs and Macqueen, 1984). Frequently, coarse-crystalline white "saddle" dolomite is observed on the walls of the resulting vugs.

Main stage of ore precipitation

The main stage of ore mineral deposition is complex and involved sulphide precipitation; solution, fracturing, and host rock collapse; the deposition of carbonate sediments in karst channelways; precipitation and replacement of dolomite in voids and fractures; and local emplacement and sulphurization of bitumen (Krebs and Macqueen, 1984; Fig. 7). The typical paragenetic sequence of the sulphide mineralization is marcasite followed by pyrite, sphalerite, and galena (Kyle, 1981). Although sphalerite is characteristically observed on the surfaces of "pre-ore" dolomite phases, there is also evidence for syngenetic precipitation of the two mineral phases, as coarse-crystalline "saddle" dolomite is commonly interlayered with sphalerite.
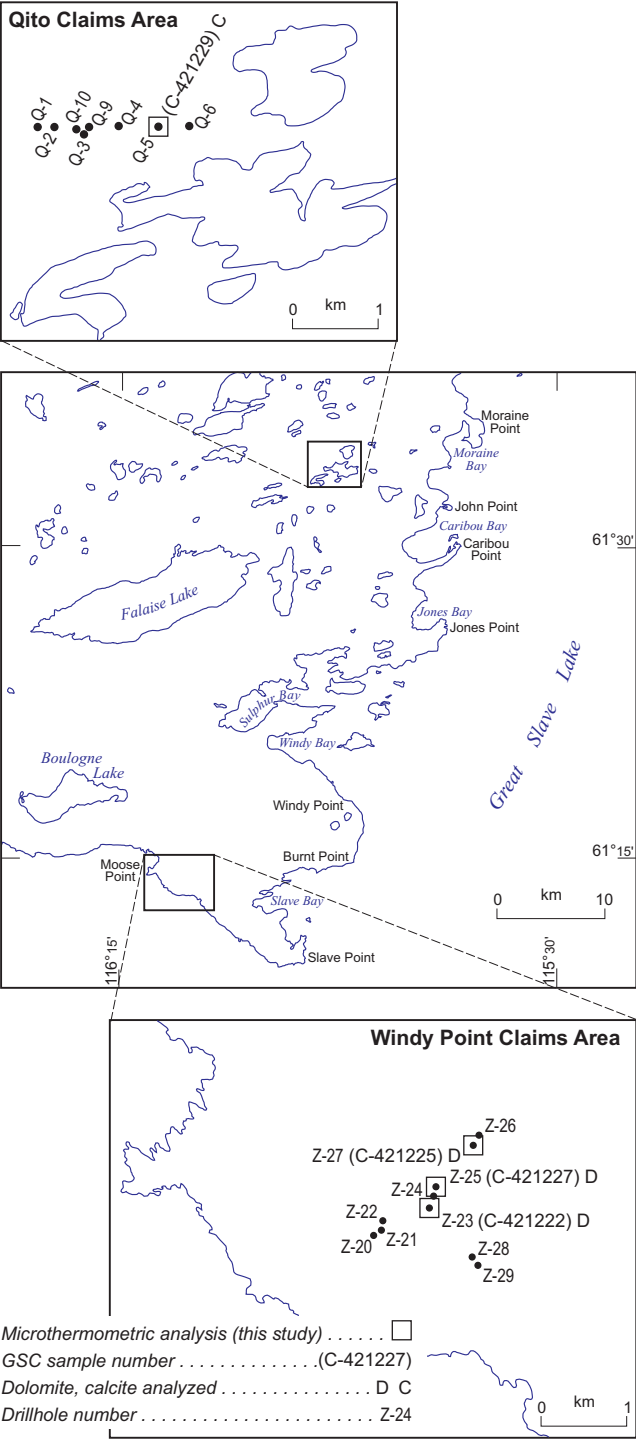
Figure 6. Drillhole locations on the western shore of Great Slave Lake, north of Hay River. Fluid inclusion microthermometry was conducted on dolomite in core from three drillholes in the former Windy Point claim area, and on calcite from core from one drillhole in the former Qito claim area. *See* Figure 2 for location.
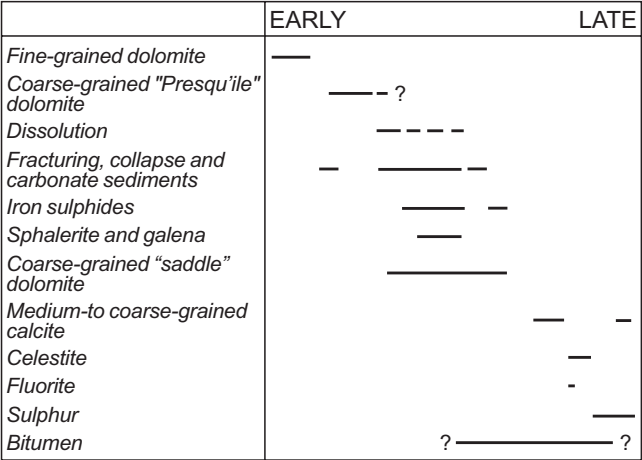
Figure 7. Generalized major paragenetic stages of the Pine Point deposit (*modified after* Kyle, 1981; and Krebs and Macqueen, 1984).

Post-ore stage

Following the main stage of ore deposition, further fracturing, dissolution, and dolomitization occurred along with sulphide remobilization, calcite, celestite, fluorite, sulphur, and bitumen emplacement (Kyle, 1981; Fig. 7). Typically, the post-ore dolomite forms as coarse "saddle" dolomite crystals along post-ore vugs and fractures, and as a late-stage precipitate on the surfaces of euhedral sphalerite crystals (Fritz, 1969; Krebs and Macqueen, 1984). The occurrence of medium- to coarse-grained white calcite (commonly equant) is restricted to the post-ore stage, and is a useful indicator because of its widespread abundance (Krebs and Macqueen, 1984).

Sample classification

In the absence of sulphide mineralization, Krebs and Macqueen (1984) reported that, with the exception of the "Pre-ore" fine-grained dolomite and "Post-ore" white calcite, it is not possible to distinguish carbonates that precipitated either prior to, or during sulphide emplacement from carbonates that formed after sulphide deposition. This factor proved to complicate this study as the majority of the core that was sampled does not contain sulphides (i.e. Hay West, Windy Point, and Qito samples). Because of this, for consistency across the study area, samples are classified by mineralogy ± grain size (i.e. coarse-grained dolomite (which includes Presqu'ile and saddle dolomite phases), medium- to coarse-grained white calcite, sphalerite, fine-grained dolomite, galena, and celestite) (Fig. 7).

METHODOLOGY

Selection criteria for fluid inclusion microthermometry

Criteria used to identify primary fluid inclusions conform to those of Roedder (1984). Specifically, those fluid inclusions observed in clusters containing similar liquid/vapour ratios and showing no evidence of forming along healed fractures, trapped between primary growth bands of the hosting mineral, or isolated from other fluid inclusions and showing no evidence of secondary origin or necking, were interpreted to be primary in origin. In the cases where primary fluid inclusions could not be identified, inclusions of pseudo-secondary or secondary origin were recorded, and their respective phase noted appropriately. In general, although pseudo-secondary and secondary fluid inclusions were observed on occasion, primary inclusions were the dominant fluid inclusion phase observed in the samples.

Analytical technique

Fluid inclusion microthermometry analyses were conducted on a THMSG600 Linkam stage at the University of Alberta. Calibration of the analytical equipment was carried out using synthetic fluid inclusion standards manufactured by Syn Flinc. Accuracy was determined to within ± 0.2°C for freezing runs and ± 2°C for heating to 300°C. Salinities were calculated from final ice melting temperatures and are reported as equivalent weight per cent NaCl (eq. wt. % NaCl) using the equation of Bodnar and Vityk (1994). Compositions of saline, $CaCl_2$-NaCl rich fluids were determined graphically using the NaCl-$CaCl_2$-H_2O ternary phase diagrams of Oakes et al. (1990, 1992).

Fluid inclusion characteristics

Two types of fluids (Type 1 and 2; described in the following section) are associated with the ore and gangue minerals in the vicinity of the Pine Point mining camp. Although both fluid types have relatively low homogenization temperatures, Type 1 is a far more saline fluid type than Type 2. The fluid inclusions that contain Type 1 and 2 fluids can be discriminated on the basis of host mineralization and inclusion size. The inclusions that contain Type 1 fluid are restricted to dolomite and sphalerite and are typically <10 μm in size (Fig. 8a, b, c), although some large fluid inclusions were observed (Fig. 8d). In contrast, those inclusions that contain Type 2 fluid are typically larger, commonly between 10 and 20 μm in at least one dimension (Fig. 8e, f), and are observed only in calcite and celestite.

RESULTS

Microthermometric analyses were conducted on fluid inclusions hosted in dolomite ± sphalerite ± calcite from 25 drill core samples and one surface sample in the study area (Fig. 2). Sample locations are shown in Figures 3 to 6, and results of the analyses are presented in histogram form in Figures 9, 10, and 11 and numerically in Appendix A. Figure 12 summarizes all of the microthermometric results (collected during this study as well as from previous studies) from the four areas examined.

Microthermometric analyses

Type 1 Fluid

Eutectic melting and recrystallization phase changes were observed in inclusions containing Type 1 fluid between -90 and -56°C, indicating the metastable to stable breakdown of salt hydrates (i.e. antarcticite) in the NaCl-$CaCl_2$-H_2O fluid ternary system (Davis et al., 1990). During further warming, two different melting reactions were observed, the first being the melting of hydrohalite between -56 and -40°C (Appendix A). This range in hydrohalite melt temperatures (Tm_{Hh}) indicates that the weight fraction NaCl (NaCl/NaCl+$CaCl_2$) is <0.1; evidence that the salt hydrates in Type 1 fluid are dominantly composed of $CaCl_2$.

Upon further heating, or at temperatures above the dissolution of hydrohalite, ice melting was observed. Ice melt temperatures (Tm_{ice}) were generally consistent between the different dolomite phases (i.e. coarse-grained "Presqu'ile" dolomite vs. coarse-grained "saddle" dolomite), however some Tm_{ice} variation was observed between sphalerite and dolomite. Sphalerite-hosted inclusions generally underwent ice melting between -35 and -21°C (ave. = -27.1°C ± 3.8 [1σ], n=42; Appendix A; Fig. 9a), whereas ice melting in dolomite-hosted inclusions typically occurred between -32 and -13°C (ave. = -24.4°C ± 5.3 [1σ], n=79; Appendix A; Fig. 10a). The average salinities of the inclusions hosted in sphalerite and dolomite (calculated in terms of weight per cent NaCl equivalent) overlap, and are 27.4 ± 2.5 [1σ] and 25.5 ± 3.7 [1σ], respectively.

Inclusions containing Type 1 fluid homogenized into the liquid phase with increased temperatures (Th_L). Two distinct Th_L populations exist for Type 1 fluid trapped in sphalerite; 53 to 67°C (ave. = 61°C ± 4.9 [1σ], n=7) for samples from the Pine Point deposits, and 85 to 112°C (ave. = 97°C ± 13.6 [1σ], n=16) for those from the Westmin property (Appendix A; Fig. 9b). A span in Th_L values is also recorded for fluid inclusions hosted in dolomite, which range from 80 to 125°C (ave. = 100°C ± 9.6 [1σ], n=82; Appendix A; Fig. 10b). The relatively low Th_L for sphalerite and dolomite may indicate these minerals formed at shallow depths and therefore an adjustment of only a few degrees is required to account for pressure correction (Roedder, 1968). The appearance of the fluid
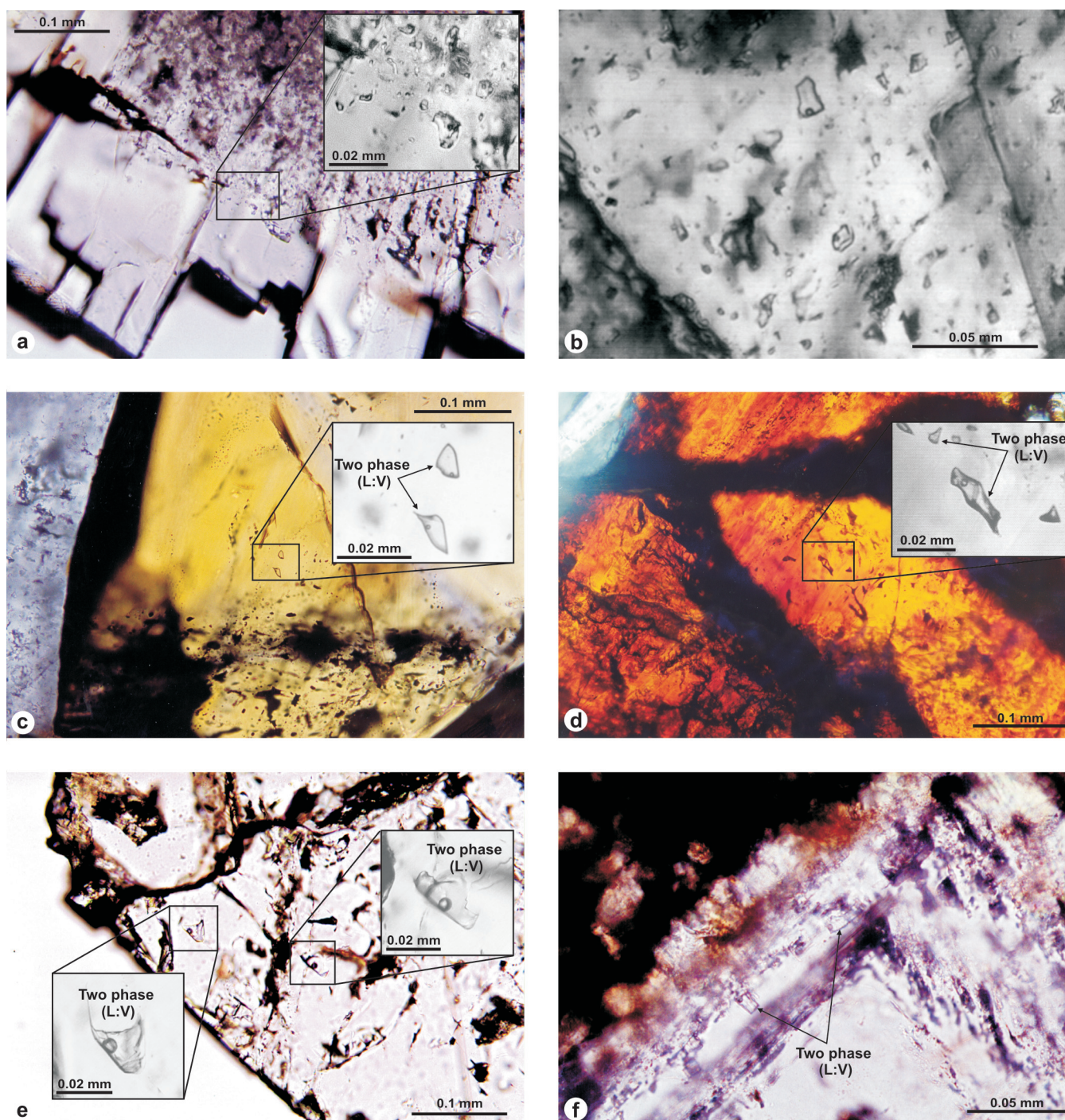
Figure 8. a. Cluster of primary, liquid-rich fluid inclusions along the edge of a dolomite crystal (sample HW-79-11-33; C-421239). Hydrohalite melting occurred between -56 and -48°C, while final ice melting ranged from -28 and -26°C. Fluid inclusion homogenization spanned from 102 to 108°C; **b.** cluster of primary, liquid-rich inclusions hosted in coarse-grained dolomite (sample O556-754-449'; C-421039). Hydrohalite melting occurred at approximately 52°C; ice melting ranged from -34.5 to -26°C. Homogenization temperatures were tightly clustered between 99 and 101°C; **c.** two isolated, saline-liquid-rich inclusions hosted in honey-yellow crystalline sphalerite from sample O556-754-507' (C-421041). Although the lower inclusion appears to have a tail, which may indicate that it has undergone post-trapping modification (i.e., leakage), both inclusions recorded similar heating behaviors: hydrohalite melting at >-50°C, final ice melting at -23°C, and vapour homogenization at 107°C; **d.** a small cluster of fluid inclusions hosted in dark crystalline sphalerite from sample P499-783-395' (C-421051). Inclusions in this sample recorded melting temperatures very similar to those in **c**, with hydrohalite melting occurring >-50°C and final ice melting at approximately -22°C. Vapour homogenization temperatures were slightly lower than those of sample C-421041, ranging from 95°C to 96°C; **e.** two isolated, liquid-rich inclusions hosted in the edge of a calcite crystal (sample N81-98-3208). Final ice melting temperatures were between -1.0 and -0.4°C for the two samples. No homogenization temperatures were determined as both samples decrepitated during the heating run; **f.** two-phase (vapour-liquid) inclusions in calcite growth band (sample Qito-Q5-27; C-421229). Inclusions showed final ice meltouts that ranged between -5.2 and -3.9°C, and homogenized to the liquid phase between 105 and 116°C.
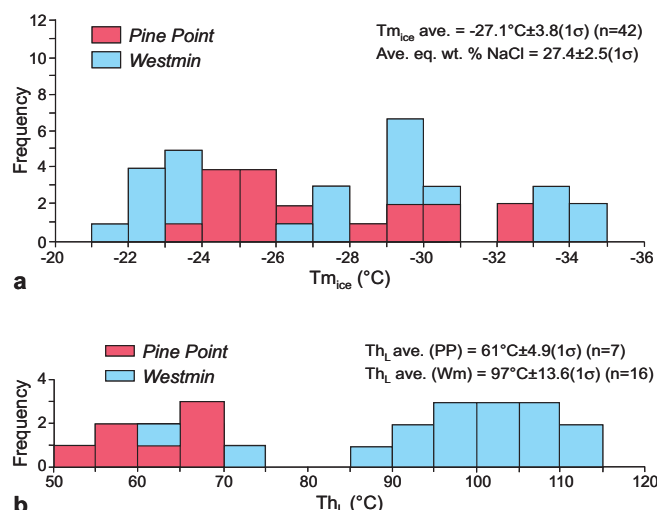
Figure 9. Histograms of microthermometric measurements of fluid inclusions in sphalerite. All fluids analyzed in the sphalerite conform to the Type 1 fluid. **a**. Histogram of final ice melting temperatures (Tm_{ice}); **b.** histogram of homogenization temperatures (Th_L).
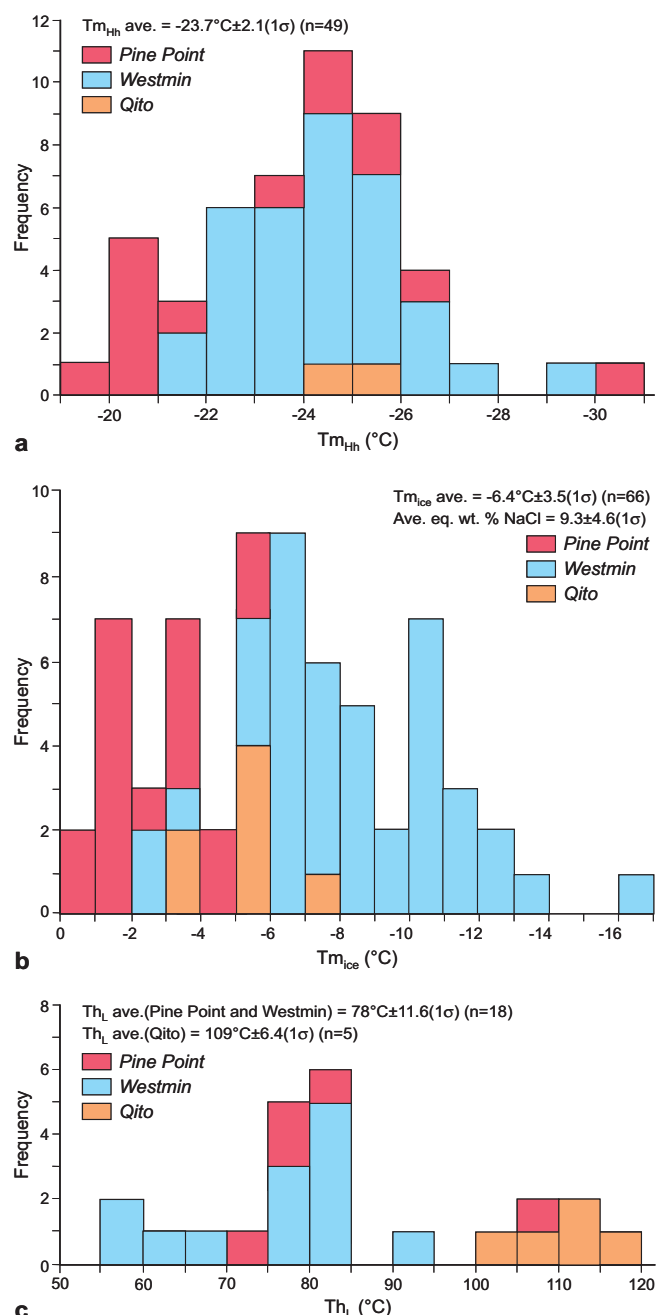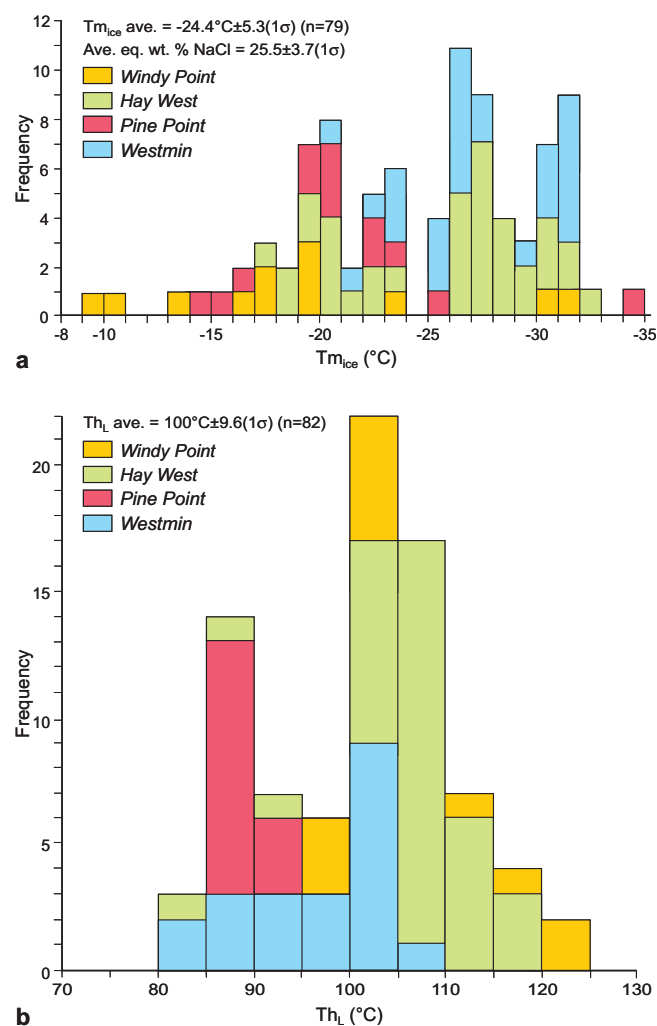
Figure 11. Histograms of microthermometric measurements of fluid inclusions in calcite. All fluids analyzed in calcite conform to the Type 2 fluid. **a**. Histogram of hydrohalite melting temperatures (Tm_{Hh}); **b.** histogram of final ice melting temperatures (Tm_{ice}); **c.** histogram of homogenization temperatures (Th_L).

Figure 10. Histograms of microthermometric measurements compiled from fluid inclusions in dolomite. All fluids analyzed in the dolomite conform to the Type 1 fluid. **a.** Histogram of final ice melting temperature (Tm_{ice}); **b.** histogram of homogenization temperatures (Th_L).
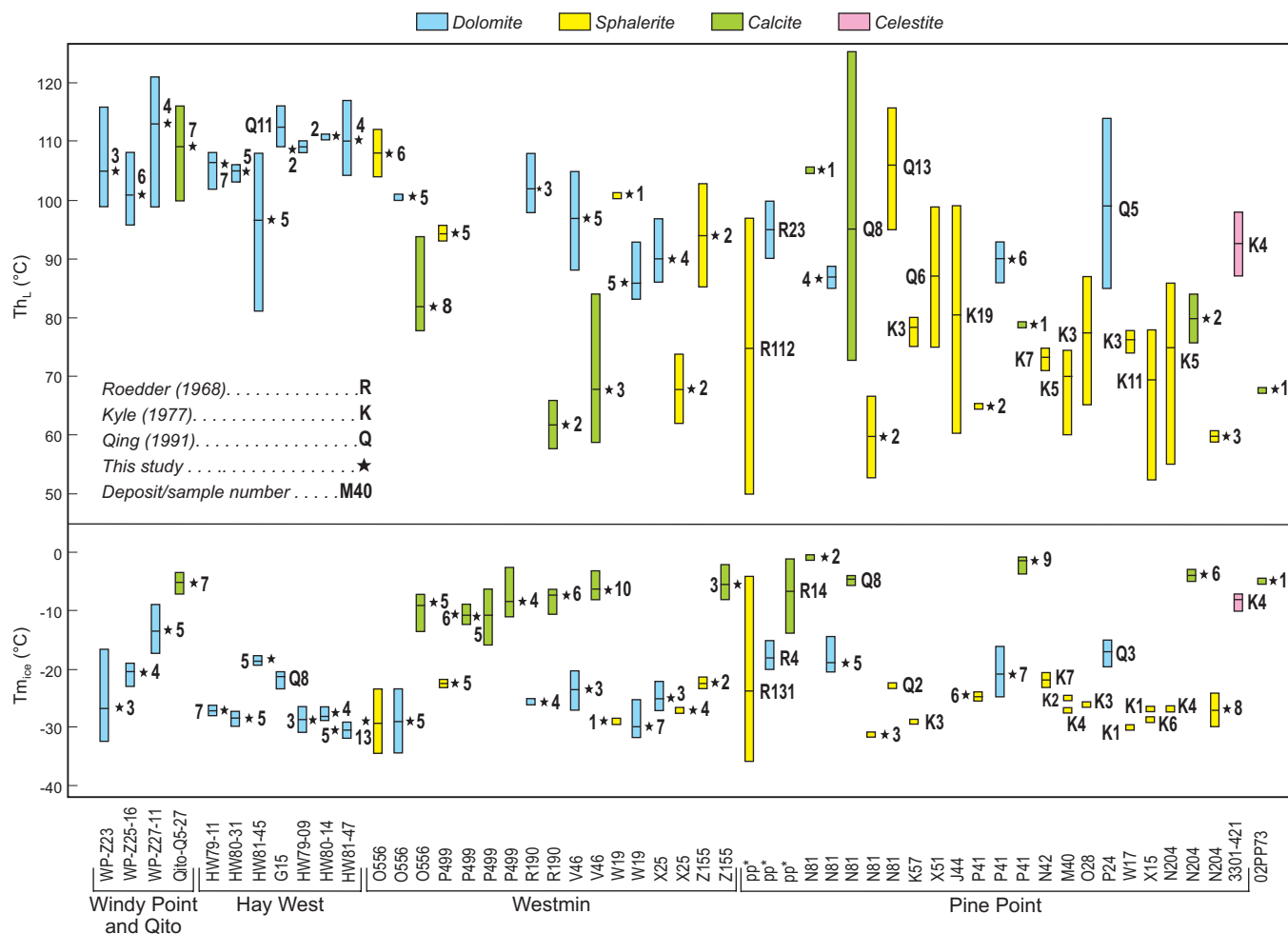
Figure 12. Ice melting temperatures (Tm$_{ice}$) and homogenization temperatures (Th$_L$) of fluid inclusions from the Pine Point, Westmin, Hay West, Windy Point, and Qito claim areas (*see* Fig. 2). In addition to the data collected in this study (indicated by stars), the data from Roedder (1968), Kyle (1977), and Qing (1991) are included. An attempt was made to present the data from west to east across the project area (Fig. 2), except for data from the Windy Point and Qito areas that are located to the north of the Hay West area. Coloured vertical bars indicate the type of mineral analyzed as well as the range of analyses; horizontal black lines represent the mean values of analyses. Beside each bar, the number of inclusions studied is indicated, as well as the reference. Kyle (1977, 1981) proposed that inclusions analyzed by Roedder (1968), (indicated by "pp*"), came from samples from Pine Point deposits N–42, O-42, and J-44.

inclusions, along with the reproducibility of the data suggests that the observed variation in Th is genuine and is not a function of post-entrapment modification of the inclusions.

Type 2 Fluid

Two phases of melting and recrystallization were constrained during cooling runs for Type 2 fluid. The first distinct phase change was the dissolution of hydrohalite (Hh), which melted over the temperature range of -28 to -19°C (ave. = -23.7°C ± 2.1 [1σ], n=49), with rare values as low as -31°C (Appendix A; Fig. 11a). This spread in the hydrohalite melting temperatures indicates that the weight fraction NaCl (NaCl/NaCl+CaCl$_2$) varies between 1 and 0.40 for Type 2 fluid. Ice melting followed the dissolution of hydrohalite and

occurred between -16 and 0°C (ave. = -6.4°C ± 3.5 [1σ], n=66; Appendix A; Fig. 11b), which constrains the average salinity (calculated in terms of weight per cent NaCl equivalent) of Type 2 fluid to 9.3 ± 4.6 [1σ].

Homogenization temperatures (Th$_L$) of Type 2 fluid form two populations: the first population spans from 58 to 105°C (ave. = 78°C ± 11.6 [1σ], n=18) and consists of analyses from Westmin and Pine Point samples, whereas the second population spans from 100 to 116°C (ave. = 109°C ± 6.40 [1σ], n=5) and is made up of analyses from the Qito area (Fig. 11c). As determined for Type 1 fluid, the overall low Th$_L$ of Type 2 fluid is supporting evidence for the trapping of fluids at relatively shallow depths, indicating that only a small temperature adjustment is required to account for pressure correction.

DISCUSSION

The composition of Type 1 fluid, as determined from primary and pseudosecondary fluid inclusions, shows very little variation in the mean hydrohalite and ice melting temperatures over the area (approx. 8,500 km^2) covered by the study (Appendix A; Fig. 12). This saline, CaCl$_2$-rich, low-temperature fluid type was observed only in sphalerite and (commonly associated) dolomite, and therefore was directly involved in the processes that deposited the metals. In contrast, Type 2 fluid consistently has lower salinities and higher NaCl to CaCl$_2$ ratios than Type 1 fluid across the study area. These data suggest that a distinctly different fluid was responsible for the deposition of sphalerite and dolomite from that of calcite and celestite. This interpretation is consistent with the observed mineral paragenesis where white calcite and celestite were precipitated later than the hydrothermal dolomite and sulphide mineralization.

Although a distinct difference was observed in the compositions of Type 1 and 2 fluids, discrimination of the two fluid types on the basis of homogenization temperature was not possible. The similarities in the relatively low homogenization temperatures may however indicate that both fluid types were trapped at relatively shallow (and potentially similar) conditions. This further suggests that the fluid conditions remained comparatively similar during the multiple events of hydrothermal mineral deposition; supportive evidence that the area in the vicinity of the Pine Point mining camp did not undergo significant tectonic instability during and after ore mineralization.

CONCLUSIONS

Microthermometric fluid analyses of gangue and sulphide minerals associated with carbonate-hosted lead-zinc mineralization to the south and west of Great Slave Lake identified two fluid types. Type 1 fluid, which occurs in dolomite and sphalerite, is a high salinity (CaCl$_2$-rich), low-temperature fluid that was directly involved in the processes that deposited the metals. Type 2 fluid, a low-temperature, moderately saline fluid type (higher weight fraction of NaCl than that of Type 1 fluid) is observed only in calcite and celestite and is not tied to the event of ore deposition. The homogenization temperatures for the two fluid types are relatively low, evidence that both fluid types were trapped at relatively near-surface conditions.

ACKNOWLEDGMENTS

REFERENCES

Bellow, J.M.
1993: Sedimentology and stratigraphy of the Alexandra Formation, Hay River region, Northwest Territories; M.Sc. thesis, University of Alberta.

Belyea, H.R. and McLaren, D.J.
1962: Upper Devonian Formations, Southern Part of Northwest Territories, Northeastern British Columbia and Northwestern Alberta; Geological Survey of Canada, Paper 61-29.

Belyea, H.R. and Norris, A.W.
1962: Middle Devonian and older Palaeozoic formations of the southern District of Mackenzie and adjacent areas; Geological Survey of Canada, Paper 62-15, 82 p.

Bodnar, R.J. and Vityk, M.O.
1994: Interpretation of microthermometric data for H$_2$O-NaCl fluid inclusions; *in* Fluid Inclusions in Minerals: Methods and Applications; (ed.) B. De Vivo and M.L. Frezzotti; published by Virginia Tech, Blacksburg, VA, p. 117–130.

Brabec, D.
1976: Geochemical soil survey Qito claims group, Mackenzie M.D., NWT; Department of Indian Affairs and Northern Development, Assessment Report No. 080440.
1981: Geochemical soil survey Qito claims property, Mackenzie Mining District, NWT. Claim: Qito 76 (B 69210). Latitude: 61°33'N, Longitude: 115°54'W; Department of Indian Affairs and Northern Development, Assessment Report No. 081315.

Cameron, A.E.
1918: Explorations in the vicinity of Great Slave Lake; Geological Survey of Canada, Summary Report 1917, Part C, p. 21C–28C.

Carter, K.M.
1980: Geological, geochemical and geophysical report for the Hay West exploration program Latitude: 60°45'N; Longitude 116°20'W, Northwest Territories; Department of Indian Affairs and Northern Development, Assessment Report No. 081224.
1981: Geological, geochemical and geophysical report for the Hay West exploration program Latitude: 60°45'N; Longitude 116°20'W, Northwest Territories; Department of Indian Affairs and Northern Development, Assessment Report No. 081483.

Davis, D.W., Lowenstein, T.K., and Spencer, R.J.
1990: Melting behavior of fluid inclusions in laboratory-grown halite crystals in the systems NaCl-H$_2$O, NaCl-KCl-H$_2$O, NaCl-MgCl$_2$-H$_2$O and NaCl-CaCl$_2$-H$_2$O; Geochimica et Cosmochimica Acta, v. 54, p. 591–601.

Douglas, R.J.W.
1959: Great Slave Lake and Trout River Map-areas, Northwest Territories, 85S 1/2 and 95A; Geological Survey of Canada, Paper 58-11, 57 p.

Douglas, R.J.W., Gabrielse, H., Wheeler, J.O., Stott, D.F., and Belyea, H.R.
1970: Geology of Western Canada; *in* Geology and Economic Minerals of Canada; Geological Survey of Canada, Economic Geology Report no. 1, p. 366–488.

Fritz, P.
1969: The oxygen and carbon isotopic composition of carbonates from the Pine Point lead-zinc ore deposits; Economic Geology, v. 64, p. 733–741.

Germundson, R.K.
1979: Geological, geochemical, geophysical report for the Tathlina exploration program (Tathlina 1 and That 2-36 Mineral Claims) centred at Long. 116°40' and 116°55' Northwest Territories (NTS 85C/15, 16; 85F2); Department of Indian Affairs and Northern Development, Assessment Report No. 081059.
1980: Geological, geochemical, geophysical report for the Tathlina exploration program (Tathlina 1 and That 2-36 Mineral Claims) Centred at Long. 116°40' and 116°55' Northwest Territories (NTS 85C/15, 16; 85F2); Department of Indian Affairs and Northern Development, Assessment Report No. 081239.

Hadley, M.G.
1987: Stratigraphy and sedimentology of Upper Devonian strata, Hay River, NWT; M.Sc. thesis, University of Alberta.

Hadley, M.G. and Jones, B.
1990: Lithostratigraphy and nomenclature of Devonian strata in the Hay River area, Northwest Territories; Bulletin of Canadian Petroleum Geology, v. 38, p. 332–356.

Hannigan, P.K.
2001: Potential for carbonate-hosted MVT deposits in Northern Alberta and Southern NWT – A Targeted Geoscience Initiative; *in* Program and Abstracts of talks and posters, 29th Yellowknife Geoscience Forum, November 21–23, 2001, p. 22–23.
2002: Potential for carbonate-hosted MVT deposits in Northern Alberta and Southern NWT – A Targeted Geoscience Initiative; *in* Calgary Mineral Exploration Group 11th Annual Calgary Mining Forum, April 24–25, 2002, p. 25–26.

Hannigan, P.K., Morrow, D.W., Miles, W.F., Paradis, S., Wilson, N., Grasby, S., and MacLean, B.C.
2002: Potential for carbonate-hosted MVT deposits in Northern Alberta and Southern NWT: new data from the targeted geoscience initiative project; *in* Program and Abstracts of talks and posters, 30th Yellowknife Geoscience Forum, November 20–22, 2002, p. 23–24.

Heal, G.E.N.
1977: Department of Indian Affairs and Northern Development, Assessment Report No. 080704.

Jamieson, E.R.
1967: The Alexandra Reef Complex (Frasnian), Hay River area, Northwest Territories, Canada. Stratigraphy, Sedimentology and Paleoecology; Ph.D. thesis, University of Reading, England.

Klein, J.
1981: Seismic investigations for the Hay West exploration program undertaken on parts of mineral claims: EL1-75, EZ 1-42, Hart 1-25, KAK 1-9, MAC 1-20, TAT 1-42, ZM 1-6. Latitude 60°45'N; Longitude: 116°20'W, Northwest Territories (NTS sheets: 85C/9,10,11,14,15,16 and 85B/12,13); Department of Indian Affairs and Northern Development, Assessment Report No. 081483.
1982: Seismic investigations for the Hay West exploration program undertaken on parts of mineral claims: EL14-19, 21-39, Hart 1-17, 19-20, 23, 26-29, 42, Hay 1-25, MAC 1-7, 9-12, 15-19, TAT 1-5, 7, 9, 11, ZM 1-6, STRAW 1-7, BERRY 1, XYL 1-6, and LAKE 1. Latitude 60°45'N; Longitude: 116°20'W, Northwest Territories; Department of Indian Affairs and Northern Development, Assessment Report No. 081460.

Krebs, W. and Macqueen, R.
1984: Sequence of diagenetic and mineralization events, Pine Point lead-zinc property, NWT; Bulletin of Canadian Petroleum Geology, v. 32, p. 434–464.

Kyle, J.R.
1977: Development of sulfide-hosted structures and mineralization, Pine Point, Northwest Territories; Ph.D. thesis, University of Western Ontario.
1981: Geology of the Pine Point lead-zinc district; *in* Handbook of Strata-Bound and Stratiform Ore Deposits, (ed.) K.H. Wolf; Elsevier Publishing Co., Amsterdam, New York, v. 9, p. 643–741.

Lane, R.W.
1980a: Windy Point Group MacKenzie M.D., NWT. Latitude: 61°15', Longitude: 116°08'. Assessment report for diamond hole drilling on mineral claims HA 346, HA 373, HA 374, HA 380, HA 381, HA 408, and MARY 516; Department of Indian Affairs and Northern Development, Assessment Report No. 081333.
1980b: Assessment report for geochemical & geophysical anomalies, Qito claims 2, 9, and 74. Latitude: 61°35', Longitude: 115°55', Mackenzie M.D., Northwest Territories; Department of Indian Affairs and Northern Development, Assessment Report No. 081238.

Lantos, J.A.
1983: Middle Devonian stratigraphy north of the Pine Point barrier complex, Pine Point, N.W.T; M.Sc. thesis, University of Alberta.

Law, J.
1955: Geology of northwestern Alberta and adjacent areas; American Association of Petroleum Geologists Bulletin, v. 39, p. 1927–1975.

Meijer Drees, N.C.
1993: The Devonian succession in the subsurface of the Great Slave and Great Bear Plains, Northwest Territories; Geological Survey Canada, Bulletin 393, 222 p.

Norris, A.W.
1965: Stratigraphy of Middle Devonian and older Paleozoic rocks of the Great Slave Lake region, Northwest Territories; Geological Survey Canada, Memoir 322.

Norris, A.W. and Uyeno, T.T.
1998: Middle Devonian brachiopods, conodonts, stratigraphy, and transgressive-regressive cycles, Pine Point area, south of Great Slave Lake, District of Mackenzie, Northwest Territories; Geological Survey of Canada, Bulletin 522, 191 p.

Oakes, C.S. Bodnar, R.J., and Simonson, J.M.
1990:   The system NaCl-CaCl$_2$-H$_2$O: I. The ice liquidous at 1 atm. Pressure; Geochimica et Cosmochimica Acta, v. 54, p. 603–610.

Oakes, C.S., Sheets, R.W., Bodnar, R.J., and Simonson, J.M.
1992:   (NaCl+CaCl$_2$){aq}: Phase equilibria and volumetric properties: (extended abstract); PACROFI IV Abstracts with Program, p. 128–132.

Qing, H.
1991:   Diagenesis of Middle Devonian Presqu'ile dolomite Pine Point NWT and adjacent subsurface; Ph.D. thesis, McGill University.

Qing, H. and Mountjoy, E.W.
1994:   Origin of dissolution vugs, caverns, and breccias in the Middle Devonian Presqu'ile Barrier, host of Pine Point Mississippi Valley-type deposits; Economic Geology, v. 89, p. 858–876.

Randall, A.W., Barr, D.A., and Giroux, G.H.
1985:   Geological Aspects of Ore Reserve Estimates, Pine Point District Zinc-Lead Deposits, N.W.T.; SME-AIME Fall Meeting Albuquerque, New Mexico, October 16-18, 1985, Preprint #85-316, 20 p.

Rasmussen, P.
1981:   Carbonate barrier-basinal shale relationships: A study of the Buffalo River shale (Middle Devonian); B.Sc. thesis, University of Waterloo.

Rhodes, D., Lantos, E.A., Lantos, J.A., Webb, R.J., and Owens, D.C.
1984:   Pine Point ore bodies and their relationship to the stratigraphy, structure, dolomitization and karstification on the Middle Devonian Barrier Complex; Economic Geology, v. 79, p. 991–1055.

Richmond, W.O.
1965:   Paleozoic stratigraphy and sedimentation of the Slave Point Formation, southern Northwest Territories and northern Alberta; Ph.D. thesis, Stanford University.

Roedder, E.
1968:   Temperature, salinity, and origin of the ore-forming fluids at Pine Point, Northwest Territories, Canada, from fluid inclusion studies; Economic Geology, v. 63, p. 439–450.
1984:   Fluid inclusions. Mineralogical Society of America, Reviews in Mineralogy, v. 12, 646 p.

Skall, H.
1975:   The paleoenvironment of the Pine Point lead-zinc district; Economic Geology, v. 70, p. 22–47.

Turner, W.A. and Gal, L.P.
2003:   Regional structural data from the Hay River area, Northwest Territories, with emphasis on the Pine Point mining camp; *in* Current Research, Part C, Geological Survey of Canada, Paper 2003-C, 10 p.

Turner, W.A., Pierce, K.L., and Cairns, K.A.
2002:   Great Slave Reef (GSR) Project Drillhole Database. A compilation of the drillhole locations, drill logs, and associated geochemical data for the Great Slave Reef Joint Venture Project; Interior Platform, Northwest Territories, Canada (NTS 85B11 to 14); C.S. Lord Northern Geoscience Centre, Yellowknife, NT, NWT Open File Report 2002-001.

Williams, G.K.
1977:   The Hay River Formation and its relationship to adjacent formations, Slave River map-area, NWT; Geological Survey of Canada, Paper 75-12, 17 p

Appendix A

Microthermometric measurements of carbonates and sphalerite from Great Slave Lake area

GSC sample #	Identification #	Host material	Inclusion analyses #	Origin	Phase	Volume H$_2$O (%)	Tm$_{Hh}$ (°C)	Wt. fraction (NaCl/NaCl+CaCl$_2$)	Tm$_{ice}$ (°C)	NaCl eq. (wt %)	Th$_L$ (°C)
C-421006	Z155-223-287'	Sphalerite	1	P	L:V	95	>-43	>0.1	-21.1	23.4	85
C-421006	Z155-223-287'	Sphalerite	2	P	L:V	95	>-43	>0.1	-23.7	25.2	103
Ave.		Sphalerite					**>-43**		**-22.4**	**24.3**	**94.0**
C-421006	Z155-223-287'	Calcite	3	P	L:V	95	-25.0	0.48	-8.3	12.1	
C-421006	Z155-223-287'	Calcite	4	P	L:V	95	-24.3	0.50	-2.1	3.5	
C-421006	Z155-223-287'	Calcite	5	P	L:V	95			-6.2	9.5	
Ave.		Calcite					**-24.7**		**-5.5**	**8.4**	
C-421014	X25-77-(444'-448')	Sphalerite	1	S	L:V	95			-26.5	27.0	74
C-421014	X25-77-(444'-448')	Sphalerite	2	S	L:V	95	-52.4	0.05	-27.5	27.6	62
C-421014	X25-77-(444'-448')	Sphalerite	3	S	L	100			-27.5	27.6	
C-421014	X25-77-(444'-448')	Sphalerite	4	S	L	100	-54.6	0.05	-27.5	27.6	
Ave.		Sphalerite					**-53.5**		**-27.3**	**27.4**	**68**
C-421014	X25-77-(444'-448')	Dolomite	1	P	L:V	95	b/w -54 & -52	0.05	-26.5	27.0	92
C-421014	X25-77-(444'-448')	Dolomite	2	P	L:V	95	b/w -54 & -52	0.05	-22.0	24.0	87
C-421014	X25-77-(444'-448')	Dolomite	3	P	L:V	95	b/w -54 & -52	0.05	-23.0	24.7	86
C-421014	X25-77-(444'-448')	Dolomite	4	P	L:V	95	b/w -54 & -52	0.05	-27.0	27.3	97
Ave.		Dolomite					**~-53**		**-24.6**	**25.7**	**90**
C-421021	V46-239-401'	Calcite	1	P	L:V	95	-24.2	0.50	-3.1	5.1	84
C-421021	V46-239-401'	Calcite	2	P	L:V	95	-25.0	0.48	-5.0	7.9	59
C-421021	V46-239-401'	Calcite	3	P	L	100	-24.0	0.56	-6.0	9.2	
C-421021	V46-239-401'	Calcite	4	P	L	100	-24.0	0.56	-7.1	10.6	
C-421021	V46-239-401'	Calcite	5	P	L:V	95	-29.0	0.27	-6.2	9.5	62
C-421021	V46-239-401'	Calcite	6	P	L:V	95	-21.3	1.00	-8.2	12.0	
C-421021	V46-239-401'	Calcite	7	P	L:V	95			-8.3	12.1	
C-421021	V46-239-401'	Calcite	8	S	L	100	-23.2	0.63	-6.1	9.3	
C-421021	V46-239-401'	Calcite	9	S	L	100	-24.3		-5.9	9.1	
C-421021	V46-239-401'	Calcite	10	S	L	100			-6.5	9.9	
Ave.		Calcite					**-24.4**		**-6.2**	**9.5**	**68**
C-421021	V46-239-401'	Dolomite	1	P	L:V	95	-56.0	0.05	-27.0	27.3	102
C-421021	V46-239-401'	Dolomite	2	P	L:V	95			-23.0	24.7	104
C-421021	V46-239-401'	Dolomite	3	P	L:V	95			-26.8	27.1	105
C-421021	V46-239-401'	Dolomite	4	P	L:V	95	-50.0	0.05	-20.0	22.7	88
C-421021	V46-239-401'	Dolomite	5	P	L:V	95	-50.0	0.05	-21.5	23.7	88
Ave.		Dolomite					**-52.0**		**-23.7**	**25.1**	**97**

Ave. = Average
wt. % = weight percent
Eq. = equivalent

Phase
L:V = two-phase inclusion (liquid + vapor)
L = monophase liquid inclusion

Temperatures
Tm$_{ice}$ = Temperature of ice melting
Tm$_{Hh}$ = Temperature of hydrohalite melting
Th$_L$ = Temperature of homogenization

Origin
P = primary inclusion
Ps = pseudosecondary inclusion
S = secondary inclusion

Appendix A (cont.)

GSC sample #	Identification #	Host material	Inclusion analyses #	Origin	Phase	Volume H$_2$0 (%)	Tm$_{Hh}$ (°C)	Wt. fraction (NaCl/NaCl+CaCl$_2$)	Tm$_{ice}$ (°C)	NaCl eq. (wt %)	Th$_L$ (°C)
C-421025	R190-750-425'	Calcite	1	P	L:V	95	-23.3	0.63	-6.6	10.0	
C-421025	R190-750-425'	Calcite	2	P	L:V	95	-23.3	0.63	-6.2	9.5	
C-421025	R190-750-425'	Calcite	3	P	L:V	95	-22.0	0.83	-6.3	9.6	
C-421025	R190-750-425'	Calcite	4	P	L:V	95	-22.3	0.78	-6.6	10.0	
C-421025	R190-750-425'	Calcite	5	P	L:V	95	-22.7	0.73			
C-421025	R190-750-425'	Calcite	6	P	L:V	95	-25.0	0.48	-11.0	15.0	58
C-421025	R190-750-425'	Calcite	7	P	L:V	95	-21.0	1.00	-8.3	12.1	66
Ave.		Calcite					**-22.8**		**-7.5**	**11.0**	**62**
C-421025	R190-750-425'	Dolomite	8	P	L:V	95	-53.0	>0.05	-25.5	26.3	
C-421025	R190-750-425'	Dolomite	9	P	L:V	95	-53.0	>0.05	-26.0	26.6	100
C-421025	R190-750-425'	Dolomite	10	P	L:V	95			-26.0	26.6	108
C-421025	R190-750-425'	Dolomite	11	P	L:V	95	-50.5	0.05	-26.0	26.6	98
Ave.		Dolomite					**-52.2**		**-25.9**	**26.6**	**102**
C-421039	O556-754-499'	Dolomite	1	P	L:V	95	-52.0	0.05	-29.8	29.1	99
C-421039	O556-754-499'	Dolomite	2	P	L:V	95			-25.5	26.3	
C-421039	O556-754-499'	Dolomite	3	P	L:V	95	-55.0	>0.05	-31.0	29.9	101
C-421039	O556-754-499'	Dolomite	4	P	L	100	-52.0	>0.05	-30.9	29.8	
C-421039	O556-754-499'	Dolomite	5	P	L:V	95	> -52	>0.05	-26.0	26.6	101
C-421039	O556-754-499'	Dolomite	6	P	L:V	95	-54.0	>0.05	-23.6	25.1	100
C-421039	O556-754-499'	Dolomite	7	P	L:V	95	-52.0	>0.05	-31.3	30.1	101
C-421039	O556-754-499'	Dolomite	8	P	L:V	95	-57.5	>0.05	-34.5	32.3	101
Ave.		Dolomite					**-53.8**		**-29.1**	**28.6**	**101**
C-421039	O556-754-499'	Calcite	1	P	L:V	95	-22.1	0.80		0.0	81
C-421039	O556-754-499'	Calcite	2	P	L:V	95			-7.8	11.5	81
C-421039	O556-754-499'	Calcite	3	P	L	100	-23.1	0.69	-7.7	11.4	
C-421039	O556-754-499'	Calcite	4	P	L:V	95	-22.8	0.73	-13.8	17.7	
C-421039	O556-754-499'	Calcite	5	P	L:V	95	-23.4	0.64	-7.4	11.0	82
C-421039	O556-754-499'	Calcite	6	P	L:V	95	-24.0	0.56			78
C-421039	O556-754-499'	Calcite	7	P	L:V	95	-26.0	0.40			78
C-421039	O556-754-499'	Calcite	8	P	L:V	95	-27.0	0.34			84
C-421039	O556-754-499'	Calcite	9	P	L:V	95	-26.0	0.40			
C-421039	O556-754-499'	Calcite	10	P	L:V	95	-23.0	0.70	-7.1	10.6	94
C-421039	O556-754-499'	Calcite	11	P	L:V	95	-24.0	0.56			78
Ave.		Calcite					**-24.1**		**-8.8**	**12.4**	**82**
C-421041	O556-754-507'	Sphalerite	1	P	L:V	95			-23.7	25.2	107
C-421041	O556-754-507'	Sphalerite	2	P	L:V	95	>-41	>0.1	-23.2	24.8	107
C-421041	O556-754-507'	Sphalerite	3	P	L:V	95	~ -53	>0.05	-23.2	24.8	
C-421041	O556-754-507'	Sphalerite	4	P	L:V	95	~ -53	>0.05	-29.2	28.7	112
C-421041	O556-754-507'	Sphalerite	5	P	L:V	95	~ -53	>0.05	-33.3	31.4	110

Appendix A (cont.)

GSC sample #	Identification #	Host material	Inclusion analyses #	Origin	Phase	Volume H₂0 (%)	Tm_Hh (°C)	Wt. fraction (NaCl/NaCl+CaCl₂)	Tm_ice (°C)	NaCl eq. (wt %)	Th_L (°C)
C-421041	O556-754-507¹	Sphalerite	6	P	L	100	~ -53	>0.05	-33.0	31.2	
C-421041	O556-754-507¹	Sphalerite	7	P	L:V	95	~ -53	>0.05	-29.0	28.5	108
C-421041	O556-754-507¹	Sphalerite	8	P	L	100	~ -53	>0.05	-33.6	31.6	
C-421041	O556-754-507¹	Sphalerite	9	P	L	100	~ -53	>0.05	-30.0	29.2	
C-421041	O556-754-507¹	Sphalerite	10	P	L	100	~ -53	>0.05	-34.0	31.9	
C-421041	O556-754-507¹	Sphalerite	11	P	L	100	~ -53	>0.05	-34.4	32.2	
C-421041	O556-754-507¹	Sphalerite	12	P	L:V	95	~ -53	>0.05	-29.4	28.8	104
C-421041	O556-754-507¹	Sphalerite	13	P	L	100	~ -53	>0.05	-29.0	28.5	
Ave.		Sphalerite					**~ -53**		**-29.6**	**29.0**	**108**
C-421049	P499-783-375¹	Calcite	1	P	L:V	95	-25.0	0.48	-2.5	4.2	
C-421049	P499-783-375¹	Calcite	2	P	L:V	95	-24.0	0.56	-9.5	13.4	
C-421049	P499-783-375¹	Calcite	3	P	L:V	95			-10.7	14.7	
C-421049	P499-783-375¹	Calcite	4	P	L:V	95			-10.0	14.0	
Ave.		Calcite					**-24.5**		**-8.2**	**11.6**	
C-421051	P499-783-395¹	Calcite	1	P	L:V	95	~(-23 to -21)	(b/w 0.7 and 1.0)	-5.9	9.1	
C-421051	P499-783-395¹	Calcite	2	P	L:V	95	~(-23 to -21)	(b/w 0.7 and 1.0)	-10.8	14.8	
C-421051	P499-783-395¹	Calcite	3	P	L:V	95	~(-23 to -21)	(b/w 0.7 and 1.0)	-10.7	14.7	
C-421051	P499-783-395¹	Calcite	4	P	L:V	95	~(-23 to -21)	(b/w 0.7 and 1.0)	-11.1	15.1	
C-421051	P499-783-395¹	Calcite	5	P	L:V	95	~(-23 to -21)	(b/w 0.7 and 1.0)	-16.0	19.6	
Ave.		Calcite					**-22**		**-10.9**	**14.7**	
C-421051	P499-783-395¹	Sphalerite	6	P	L:V	95	>53 deg C	>0.05	-22.0	24.0	96
C-421051	P499-783-395¹	Sphalerite	7	P	L:V	95			-22.1	24.1	93
C-421051	P499-783-395¹	Sphalerite	8	P	L:V	95			-22.0	24.0	96
C-421051	P499-783-395¹	Sphalerite	9	P	L:V	95			-22.0	24.0	95
C-421051	P499-783-395¹	Sphalerite	10	P	L:V	95			-23.1	24.8	93
Ave.		Sphalerite					**>53**		**-22.2**	**24.2**	**94.5**
C-421053	P499-783-398¹	Calcite	1	P	L:V	95			-12.0	16.0	
C-421053	P499-783-398¹	Calcite	2	P	L:V	95	-25.0	0.48	-9.5	13.4	
C-421053	P499-783-398¹	Calcite	3	P	L:V	95			-11.0	15.0	
C-421053	P499-783-398¹	Calcite	4	P	L:V	95	-26.0	0.40	-8.8	12.7	
C-421053	P499-783-398¹	Calcite	5	P	L:V	95	-25.0	0.48	-12.3	16.3	
C-421053	P499-783-398¹	Calcite	6	P	L:V	95	-22.6	0.74	-10.0	14.0	
C-421053	P499-783-398¹	Calcite	7	P	L:V	95			-10.0	14.0	
C-421053	P499-783-398¹	Calcite	8	P	L:V	95			-10.0	14.0	
Ave.		Calcite					**-24.5**		**-10.5**	**14.4**	

Ave. = Average
wt. % = weight percent
Eq. = equivalent

Phase
L:V = two-phase inclusion (liquid + vapor)
L = monophase liquid inclusion

Temperatures
Tm_ice = Temperature of ice melting
Tm_Hh = Temperature of hydrohalite melting
Th_L = Temperature of homogenization

Origin
P = primary inclusion
Ps = pseudosecondary inclusion
S = secondary inclusion

Appendix A (cont.)

GSC sample #	Identification #	Host material	Inclusion analyses #	Origin	Phase	Volume H₂0 (%)	Tm_Hh (°C)	Wt. fraction (NaCl/NaCl+CaCl₂)	Tm_ice (°C)	NaCl eq. (wt %)	Th_L (°C)
C-421062	W19-219-(465'-470')	Saddle dolomite	1	P	L:V	95	>-50	0.05	-31.8	30.4	85
C-421062	W19-219-(465'-470')	Saddle dolomite	2	P	L	100	>-50	0.05	-31.2	30.0	
C-421062	W19-219-(465'-470')	Saddle dolomite	3	P	L:V	95	>-50	0.05	-31.0	29.9	83
C-421062	W19-219-(465'-470')	Saddle dolomite	4	P	L:V	95	>-50	0.05	-30.3	29.4	87
C-421062	W19-219-(465'-470')	Saddle dolomite	5	P	L:V	95	>-50	0.05	-30.0	29.2	90
C-421062	W19-219-(465'-470')	Saddle dolomite	6	P	L:V	95	>-50	0.05	-31.0	29.9	80
C-421062	W19-219-(465'-470')	Saddle dolomite	7	P	L:V	95	>-50		-25.0	26.0	93
Ave.							**>-50**		**-30.0**	**29.2**	**86**
C-421062	W19-219-(465'-470')	Sphalerite	1	P	L:V	95	**>-50**	0.05	**-29.0**	**28.5**	**101**
C-421222	WP-Z23	Dolomite	1	P	L:V	95	-41.6	0.10	-30.0	29.2	102
C-421222	WP-Z23	Dolomite	2	P	L:V	95	>-50		-16.5	20.0	116
C-421222	WP-Z23	Dolomite	3	P	L:V	95	>-50	0.05	-31.5	30.2	99
Ave.		**Dolomite**					**~-50**		**-26.8**	**27.0**	**105**
C-421225	WP-Z27-11	Dolomite	1	?	L:V	95			-13.8	17.7	121
C-421225	WP-Z27-11	Dolomite	2	?	L:V	95			-9.0	12.9	121
C-421225	WP-Z27-11	Dolomite	3	P	L:V	95	-49.0	0.05	-17.3	20.7	99
C-421225	WP-Z27-11	Dolomite	4	?	L	100	-56.0	>0.05	-10.5	14.5	
C-421225	WP-Z27-11	Dolomite	5	P	L:V	95	-50.0	0.05	-17.5	20.8	110
Ave.		**Dolomite**					**-51.7**		**-13.6**	**17.3**	**113**
C-421227	WP-Z25-16	Dolomite	1	P	L:V	95	>-50	0.05	-19.0	21.9	>125
C-421227	WP-Z25-16	Dolomite	2	P	L:V	95	-47.0	~-0.05	-19.5	22.3	103
C-421227	WP-Z25-16	Dolomite	3	P	L:V	95	-47.8	~-0.05	-19.3	22.2	108
C-421227	WP-Z25-16	Dolomite	4	P	L:V	95	-47.9	~-0.05	-23.1	24.8	96
C-421227	WP-Z25-16	Dolomite	5	P	L:V	95					100
C-421227	WP-Z25-16	Dolomite	6	P	L:V	95					100
C-421227	WP-Z25-16	Dolomite	7	P	L:V	95					100
Ave.		**Dolomite**					**-47.6**		**-20.2**	**22.8**	**101**
C-421229	Qito-Q5-27	Calcite	1	P	L:V	95			-3.9	6.3	112
C-421229	Qito-Q5-27	Calcite	2	P	L:V	95			-7.6	11.2	116
C-421229	Qito-Q5-27	Calcite	3	P	L:V	95	-25.6	0.43	-5.2	8.1	105
C-421229	Qito-Q5-27	Calcite	4	P	L:V	95	-24.1	0.54	-5.2	8.1	
C-421229	Qito-Q5-27	Calcite	5	P	L:V	95			-5.2	8.1	

Appendix A (cont.)

GSC sample #	Identification #	Host material	Inclusion analyses #	Origin	Phase	Volume H₂0 (%)	Tm$_{Hh}$ (°C)	Wt. fraction (NaCl/NaCl+CaCl$_2$)	Tm$_{ice}$ (°C)	NaCl eq. (wt %)	Th$_L$ (°C)
C-421229	Qito-Q5-27	Calcite	6	P	L:V	95			-5.2	8.1	112
C-421229	Qito-Q5-27	Calcite	7	P	L:V	95			-3.3	5.4	100
Ave.		**Calcite**					**-24.9**		**-5.1**	**7.9**	**109**
C-421231	HW-80-29-11	Dolomite	1	P	L:V	95	-43.0	0.10	-22.5	24.4	94
C-421231	HW-80-29-11	Dolomite	2	P	L:V	95	not observed		-22.0	24.0	110
C-421231	HW-80-29-11	Dolomite	3	P	L:V	95	not observed		-21.0	23.4	102
C-421231	HW-80-29-11	Dolomite	4	P	L:V	95	-45.0	>0.1	-20.3	22.9	111
C-421231	HW-80-29-11	Dolomite	5	P	L:V	95	~ -43	0.10	-20.5	23.0	110
C-421231	HW-80-29-11	Dolomite	6	P	L:V	95	-40.0	0.11	-20.6	23.1	110
C-421231	HW-80-29-11	Dolomite	7	P	L:V	95	-40.0	0.11	-20.5	23.0	110
C-421231	HW-80-29-11	Dolomite	8	P	L:V	95	not observed		-23.0	24.7	not observed
Ave.		**Dolomite**					**-42.0**		**-21.3**	**23.6**	**107**
C-421234	HW 79-09-20	Dolomite	1	P	L:V	95	> -53	>0.05	-28.0	27.9	108
C-421234	HW 79-09-20	Dolomite	2	P	L:V	95	> -53	>0.05	-31.0	29.9	110
C-421234	HW 79-09-20	Dolomite	3	P	L:V	95	> -53	>0.05	-26.3	26.8	109
Ave.		**Dolomite**					**> -53**		**-28.4**	**28.2**	**109.1**
C-421236	HW 80-31-14	Dolomite	1	P	L:V	95	~ -57	>0.05	-27.0	27.3	103
C-421236	HW 80-31-14	Dolomite	2	P	L:V	95	~ -57	>0.05	-27.0	27.3	105
C-421236	HW 80-31-14	Dolomite	3	P	L:V	95	~ -57	>0.05	-30.0	29.2	106
C-421236	HW 80-31-14	Dolomite	4	P	L:V	95	~ -57	>0.05	-26.9	27.2	103
C-421236	HW 80-31-14	Dolomite	5	P	L:V	95	~ -57	>0.05	-27.8	27.8	103
Ave.		**Dolomite**					**~ -57**		**-27.7**	**27.7**	**104.0**
C-421238	HW 80-14-29	Dolomite	6	P	L:V	95	~ -57	>0.05	-26.3	26.8	108
C-421238	HW 80-14-29	Dolomite	7	P	L:V	95			-28.3	28.1	109
C-421238	HW 80-14-29	Dolomite	8	P	L	100	~ -53	>0.05	-28.5	28.2	
C-421238	HW 80-14-29	Dolomite	9	P	L	100			-29.0	28.5	
Ave.		**Dolomite**					**~ -55**		**-28.0**	**27.9**	**108.5**
C-421239	HW 79-11-33	Dolomite	1	P	L:V	95	-49.0	>0.05	-26.5	27.0	108
C-421239	HW 79-11-33	Dolomite	2	P	L:V	95	-50.0	>0.05	-27.0	27.3	107
C-421239	HW 79-11-33	Dolomite	3	P	L:V	95	-52.0	>0.05	-27.0	27.3	107
C-421239	HW 79-11-33	Dolomite	4	P	L:V	95	-55.0	>0.05	-28.0	27.9	108
C-421239	HW 79-11-33	Dolomite	5	P	L:V	95	-56.0	>0.05	-26.0	26.6	107
C-421239	HW 79-11-33	Dolomite	6	P	L:V	95	-48.0	>0.05	-27.0	27.3	102

Ave. = Average
wt. % = weight percent
Eq. = equivalent

Phase
L:V = two-phase inclusion (liquid + vapor)
L = monophase liquid inclusion

Temperatures
Tm$_{Ice}$ = Temperature of ice melting
Tm$_{Hh}$ = Temperature of hydrohalite melting
Th$_L$ = Temperature of homogenization

Origin
P = primary inclusion
Ps = pseudosecondary inclusion
S = secondary inclusion

Appendix A (cont.)

GSC sample #	Identification #	Host material	Inclusion analyses #	Origin	Phase	Volume H2O (%)	TmHh (°C)	Wt. fraction (NaCl/NaCl+CaCl2)	TmIce (°C)	NaCl eq. (wt %)	ThL (°C)
C-421239	HW 79-11-33	Dolomite	7	P	L:V	95	-48.0	>0.05	-27.0	27.3	105
Ave.		**Dolomite**					**-51.1**		**-26.9**	**27.2**	**106.3**
C-421244	HW-81-45-17	Dolomite	1	P	L:V	95	-40.0	0.11	-17.7	21.0	81
C-421244	HW-81-45-17	Dolomite	2	P	L:V	95	-47.0	0.05	-19.0	21.9	105
C-421244	HW-81-45-17	Dolomite	3	P	L:V	95	~48	0.05	-18.5	21.6	100
C-421244	HW-81-45-17	Dolomite	4	P	L:V	95	~48	0.05	-19.0	21.9	108
C-421244	HW-81-45-17	Dolomite	5	P	L:V	95	~47	0.05	-18.5	21.6	89
Ave.		**Dolomite**					**~47**		**-18.5**	**21.6**	**96.7**
C-421245	HW-81-47-3	Dolomite	1	P	L:V	95	-50.0	0.05	-30.0	29.2	105
C-421245	HW-81-47-3	Dolomite	2	P	L:V	95	-50.5	0.05	-30.0	29.2	104
C-421245	HW-81-47-3	Dolomite	3	P	L:V	95			-31.5	30.2	117
C-421245	HW-81-47-3	Dolomite	4	P	L:V	95					117
C-421245	HW-81-47-3	Dolomite	5	P	L:V	95			-32.2	30.7	102
C-421245	HW-81-47-3	Dolomite	6	P	L:V	95	-51.1	0.05	-29.5	28.9	115
Ave.		**Dolomite**					**-50.5**		**-30.6**	**29.6**	**110**
	N81-65-0249	Dolomite	1	P	L:V	95	-38.0	0.13	-14.2	18.1	85
	N81-65-0249	Dolomite	2	P	L:V	95	-38.0	0.13	-20.0	22.7	89
	N81-65-0249	Dolomite	3	P	L	100	-37.0	0.13	-20.2	22.8	
	N81-65-0249	Dolomite	4	P	L:V	95	-40.0	0.11	-20.3	22.9	86
	N81-65-0249	Dolomite	5	P	L:V	95	-39.0	0.11	-19.3	22.2	89
Ave.		**Dolomite**					**-38.4**		**-18.8**	**21.7**	**87**
	N81-98-3208-B	Calcite	1	Ps	L:V	95			-1.0	1.7	105
	N81-98-3208-B	Calcite	2	Ps	L:V	95.0			-0.4	0.7	
Ave.		**Calcite**							**-0.7**	**1.2**	**105**
	N81-98-3208-B	Sphalerite	1	Ps	L	100	not observed		-32.0	30.5	
	N81-98-3208-B	Sphalerite	2	Ps	L:V	95	>-52	>0.05	not seen		53
	N81-98-3208-B	Sphalerite	3	Ps	L:V	95	>-52	>0.05	-30.8	29.7	67
	N81-98-3208-B	Sphalerite	4	Ps	L	100	>-52	>0.05	-32.0	30.5	
Ave.		**Sphalerite**					**>-52**		**-31.6**	**30**	**60**
	P41	Dolomite	1	P	L:V	95	-43.0	0.09	-25.0	26.0	92
	P41	Dolomite	2	P	L:V	95	-41.0	0.10	-15.8	19.5	89
	P41	Dolomite	3	P	L:V	95	-39.0	0.11	-16.0	19.6	
	P41	Dolomite	4	P	L:V	95	-43.0	0.09	-22.5	24.4	93
	P41	Dolomite	5	P	L:V	95	-43.0	0.09	-23.8	25.2	86
	P41	Dolomite	6	P	L:V	95	-43.0	0.09	-19.1	22.0	92
	P41	Dolomite	7	P	L:V	95	-42.0	0.09	-22.4	24.3	89
Ave.		**Dolomite**					**-42.0**		**-20.7**	**23.0**	**90**
	P41	Sphalerite	1	Ps	L	100	-50.0	0.05	-25.5	26.3	

Appendix A (cont.)

GSC sample #	Identification #	Host material	Inclusion analyses #	Origin	Phase	Volume H$_2$0 (%)	Tm$_{Hh}$ (°C)	Wt. fraction (NaCl/NaCl+CaCl$_2$)	Tm$_{Ice}$ (°C)	NaCl eq. (wt %)	Th$_L$ (°C)
	P41	Sphalerite	2	Ps	L	100	-50.0	0.05	-24.0	25.4	
	P41	Sphalerite	3	Ps	L:V	95	> -40	>.11	-24.2	25.5	65
	P41	Sphalerite	4	Ps	L	100	-50.0	0.05	-23.9	25.3	
	P41	Sphalerite	5	Ps	L:V	95	-50.0	0.05	-25.0	26.0	65
	P41	Sphalerite	6	Ps	L	100	-50.0	0.05			
	P41	Sphalerite	7	Ps	L	100			-25.5	26.3	
Ave.		Sphalerite					**-50.0**		**-24.7**	**25.8**	**65**
	P41	Calcite	1	S	L	100	-20.6	1.00	-1.3	2.2	
	P41	Calcite	2	S	L:V	95	-20.7	1.00	-2.0	3.4	79
	P41	Calcite	3	S	L	100	-19.7	1.00	-3.9	6.3	
	P41	Calcite	4	S	L	100	-20.6	1.00	-1.5	2.6	
	P41	Calcite	5	S	L	100			-1.5	2.6	
	P41	Calcite	6	S	L	100	-20.2	1.00	-1.5	2.6	
	P41	Calcite	7	S	L	100	-23.4	0.62	-1.3	2.2	
	P41	Calcite	8	S	L	100	-21.3	1.00	-0.7	1.2	
	P41	Calcite	9	S	L	100	-20.6	1.00	-1.0	1.7	
Ave.		Calcite					**-21.4**		**-1.6**	**2.8**	**79**
	N204-340-A	Sphalerite	1	Ps	L:V	95	-59.5	0.05	-28.2	28.0	59
	N204-340-A	Sphalerite	2	Ps	L:V	95	-59.0	0.05	-29.5	28.9	61
	N204-340-A	Sphalerite	3	Ps	L:V	95	not observed		-29.0	28.5	59
	N204-340-A	Sphalerite	4	P	L	100	> - 60	0.05	-24.3	25.5	
	N204-340-A	Sphalerite	5	P	L	100	> - 60	0.05	-26.1	26.7	
	N204-340-A	Sphalerite	6	P	L	100	> - 60	0.05	-24.7	25.8	
	N204-340-A	Sphalerite	7	P	L	100	> - 60	0.05	-25.0	26.0	
	N204-340-A	Sphalerite	8	P	L	100	> - 60	0.05	-30.2	29.3	
Ave.		Sphalerite					**> - 60**		**-27.1**	**27.4**	**60**
	N204-340-b	Calcite	1	S	L:V	95	-26.0	0.40	-5.3	8.3	
	N204-340-b	Calcite	2	S	L	100	-24.0	0.56	-5.0	7.9	
	N204-340-b	Calcite	3	S	L:V	95	-25.0	0.48	-3.0	4.9	
	N204-340-b	Calcite	4	S	L	100	-24.0	0.56	-4.3	6.9	
	N204-340-b	Calcite	5	S	L:V	95	-25.0	0.48	-3.9	6.3	84
	N204-340-b	Calcite	6	S	L:V	95	not observed		-3.0	4.9	76
Ave.		Calcite					**-24.8**		**-4.1**	**6.5**	**80**
	02PP73	Calcite	1	P	L:V	95	~ - 32 to -29	~0.26	-4.9	7.7	**72**

Ave. = Average
wt. % = weight percent
Eq. = equivalent

Phase
L:V = two-phase inclusion (liquid + vapor)
L = monophase liquid inclusion

Temperatures
Tm$_{Ice}$ = Temperature of ice melting
Tm$_{Hh}$ = Temperature of hydrohalite melting
Th$_L$ = Temperature of homogenization

Origin
P = primary inclusion
Ps = pseudosecondary inclusion
S = secondary inclusion